Remote Sensing Applications: Society and Environment 23 (2021) 100554

Contents lists available at ScienceDirect

Remote Sensing Applications: Society and Environment

journal homepage: www.elsevier.com/locate/rsase

Towards a workflow for operational mapping of *Aedes aegypti* at urban scale based on remote sensing

Verónica Andreo [a,b,*,1], Pablo Fernando Cuervo [b,c,1], Ximena Porcasi [a], Laura Lopez [d], Claudio Guzman [d], Carlos M. Scavuzzo [a]

[a] *Instituto de Altos Estudios Espaciales "Mario Gulich". Universidad Nacional de Córdoba (UNC), Comisión Nacional de Actividades Espaciales (CONAE), Ruta Provincial C45 Km 8. Falda del Cañete, Córdoba, Argentina*
[b] *Consejo Nacional de Investigaciones Científicas y Técnicas (CONICET), Buenos Aires, Argentina*
[c] *Laboratorio de Ecología de Enfermedades. Instituto de Ciencias Veterinarias del Litoral (ICIVET - Litoral). Universidad Nacional del Litoral (UNL), Esperanza, Santa Fe, Argentina*
[d] *Programa de Zoonosis, Área de Epidemiología, Ministerio de Salud de la Provincia de Córdoba, Córdoba, Argentina*

ARTICLE INFO

Keywords:
Dengue fever
Species distribution models
Remote sensing
Operative systems

ABSTRACT

Remote sensing (RS) applications for vector borne diseases are a field of high social impact increasingly relevant in the context of a higher frequency of Dengue, Chikungunya and Zika outbreaks at global scale and especially in Latin America. The operative use of RS technologies is however still rare. Therefore, the objective of this work is to generate and analyze multitemporal *Aedes aegypti*'s suitability maps and to share the open source tools used towards the building of an operative workflow. As a proof of concept, we implemented a process chain to obtain maps for *Ae. aegypti* activity within the 2017–2018 mosquito breeding season based on ovitraps records and RS data within the framework of ecological niche modeling. The workflow was carefully thought as to consider possible biases in training data, model calibration to attain the best hyper-parameter combination, model selection, variable selection and validation with independent data. The predictive maps showed high suitability for *Ae. aegypti* within the city, except in large vegetated areas and the commercial downtown consistently with previous studies and our own observations. Relevant variables included distance to built-up surfaces, distance to vegetated areas and correlation, a texture measure reflecting surface heterogeneity. Validation results suggested that the spatial distribution of ovitraps should be re-examined. All the steps in the proposed workflow were implemented using freely available and open source software, which warrants reproducibility and allows for re-use and modifications in terms of methods and RS or mosquito data available.

1. Introduction

Mosquitoes are responsible for several human vector-borne diseases (VBD) around the world including malaria, West Nile fever, dengue fever, zika, chikungunya and yellow fever. *Aedes aegypti*, a mosquito originally from Africa, is the main vector of the causative agents of the four latter diseases (Souza-Neto et al., 2019). In recent decades, favoured by global warming, urbanization, globalization, trade and human migration, *Ae. aegypti* has invaded many temperate areas of the world (Vezzani and Carbajo, 2008; Gubler, 2011; Liu-Helmersson et al., 2019), reaching latitudes as south as 40°S (Rubio et al., 2020). This mosquito species is fully adapted to urban areas where it can fulfill important ecological needs living alongside humans (Powell and Tabachnick, 2013). Urban areas provide water for immature stage development, blood for female reproduction and shelter that protects larvae and adults against harsh climatic conditions (Cheong, 1967; Wilke et al., 2019).

Among the VBD transmitted by *Ae. aegypti*, dengue fever causes the greatest human disease burden, with an estimated 10,000 deaths and 100,000 million symptomatic infections per year in over 125 countries (53% of the global population at risk) (Stanaway et al., 2016). The incidence of dengue has grown dramatically in recent decades, with a concomitant increasing frequency of outbreaks in South America during

* Corresponding author. Instituto de Altos Estudios Espaciales "Mario Gulich", Universidad Nacional de Córdoba (UNC), Comisión Nacional de Actividades Espaciales (CONAE), Ruta Provincial C45 Km 8. Falda del Cañete, Córdoba, Argentina.
E-mail address: veronica.andreo@ig.edu.ar (V. Andreo).
[1] These authors contributed equally to this work.

https://doi.org/10.1016/j.rsase.2021.100554
Received 30 July 2020; Received in revised form 30 October 2020; Accepted 27 May 2021
Available online 2 June 2021

the past 10 years (Bhatt et al., 2013). Two of the largest dengue outbreaks in Argentina occurred in 2009 and 2016, affecting more than 25, 900 and 56,800 people respectively, and reaching highly populated cities from temperate regions like Córdoba and Buenos Aires (Seijo et al., 2009; Estallo et al., 2014; Rotela et al., 2017). Prevention of mosquito-borne diseases like dengue, is mainly based on vector control and continuous entomological surveillance to estimate the potential risk for virus transmission and disease (Bowman et al., 2016). The prevention programs are therefore typically focused on monitoring, removal of *Ae. aegypti* breeding sites to eliminate vector larval stages, treatment of larval habitats and insecticidal spraying to reduce adult density (Getis et al., 2003).

The spatial distribution of vectors is often used as an indicator of where disease outbreaks are likely to occur in human populations (Ostfeld et al., 2005). Nowadays, Earth observation (EO) satellites constitute a basic source of environmental information used to relate to vector data within the framework of landscape epidemiology and ecological niche modeling (ENM) in order to produce potential distribution maps (Ostfeld et al., 2005; Kalluri et al., 2007; Soucy et al., 2018; de Santana Martins Rodgers et al., 2019). Given its public health relevance, many studies have addressed the distribution of *Ae. aegypti* and its environmental drivers. Most of them have focused on global and regional scales using mostly climatic predictors and medium to coarse resolution EO data (Moreno-Madriñán et al., 2014; Kraemer et al., 2015, 2019; Johnson et al., 2017). Different studies have also mapped the distribution of *Ae. aegypti* at local scales in urban areas. However, with some exceptions (e.g. Arboleda et al., 2012; Rojas et al., 2017), most of them have produced static or unique maps that either consider only a couple of months of surveillance or aggregate a full year (or several years) of mosquito data (Espinosa et al., 2016a; Rotela, 2013; Estallo et al., 2018; Albrieu-Llinás et al., 2018). Meanwhile, practitioners need operative, detailed and timely information within each season as to decide when and where to intensify surveillance or intervene with control activities as to prevent potential disease outbreaks.

In this context, and after two large dengue outbreaks, the authorities of the Health Ministry of Córdoba province, similarly to other urban areas in Argentina and Latin America, started a weekly monitoring of *Ae. aegypti* oviposition activity. To generate control strategies they required various fine resolution maps within the transmission season instead of relying on a single static distribution map. Those maps are typically produced *ad hoc* by academic support teams, following different approaches and using different sources of environmental data.

Therefore, the objective of this contribution is to generate and analyze multitemporal *Aedes aegypti*'s suitability maps and to share the open source tools used towards the building of an operative workflow that can be readily updated with incoming new mosquito and environmental data. As a proof of concept, we modelled and mapped the potential distribution of *Ae. aegypti* for three dates in the 2017–2018 mosquito season in Córdoba city, using data from ovitraps and high resolution imagery within the framework of ecological niche modeling. This framework has demonstrated to be a useful complementary tool to entomological indicators for Dengue risk assessment and prediction (Arboleda et al., 2012; Barbosa et al., 2014; Cromwell et al., 2017).

2. Materials and methods

2.1. Study area

Based on its geographic, climatic and demographic features and also on vector data availability, we chose Córdoba city as the pilot area for our study. Córdoba is the second largest city in Argentina with a population of 1,330,023 inhabitants in 2010 (INDEC, 2010). It has a surface of 576 km^2 and it is located at 31°24′ S, 64°11' W, with elevations ranging 360–480 m.a.s.l. Córdoba city has a temperate climate, with mean annual precipitation of 800 mm. The winter is markedly dry and most precipitation occurs during summer months. The rainy season spans between October and March, with the highest precipitations occurring from December to February. The mean annual temperature is 21 °C (range 12–38 °C). Winters are temperate, with several frost days in June and July (Servicio Meteorologico Nacional, 2019). The Suquía River, its tributary La Cañada and numerous other water channels run through the city. Human activities have resulted in a landscape characterized by a highly developed urban core represented by buildings and 0.66 km^2 of green areas in the form of urban parks. Suburban areas are characterized by residential neighbourhoods, mainly single-family houses with yards, interspersed with parks and other green spaces. The urban area is surrounded by agricultural fields and very small forest patches (Fig. 1).

2.2. Data

2.2.1. Entomological data

Entomological data consisted of 300 ovitraps distributed in 150 houses over 5 different areas of the city (Fig. 1). This redundancy, i.e., two traps per house, decreases the probability of accidental data loses. Houses with ovitraps were at least 150 m apart, with an average minimum distance of 350 m. Two ovitraps were placed in the front yard of each house, usually in shaded places and below or close to bushes or pots with plants. The possibility of trap installation depended on householders' written consent. Each ovitrap consisted of a black 1000 ml plastic container filled with 250 ml of tap water and a wooden paddle (15 × 2 cm) partially submerged and held vertically to serve as substrate for mosquito oviposition (Espinosa et al., 2018). Ovitraps were checked and replaced every week, starting from September 2017. Eggs laid in each wooden paddle were counted under magnifying glass.

Since ovitraps are always placed in the same locations, we could not use them for validation purposes. Instead, we used a different and independent data set consisting of larval surveys performed monthly in different neighbourhoods of the city. In these surveys, the presence of larvae in domestic containers both inside and outside households was recorded. Larvae found were collected and transported to the laboratory where they were kept until adult emergence. If at least one *Ae. aegypti* adult per sample was detected, that house was considered positive.for taxonomic identification. Houses with at least one container with *Ae.*

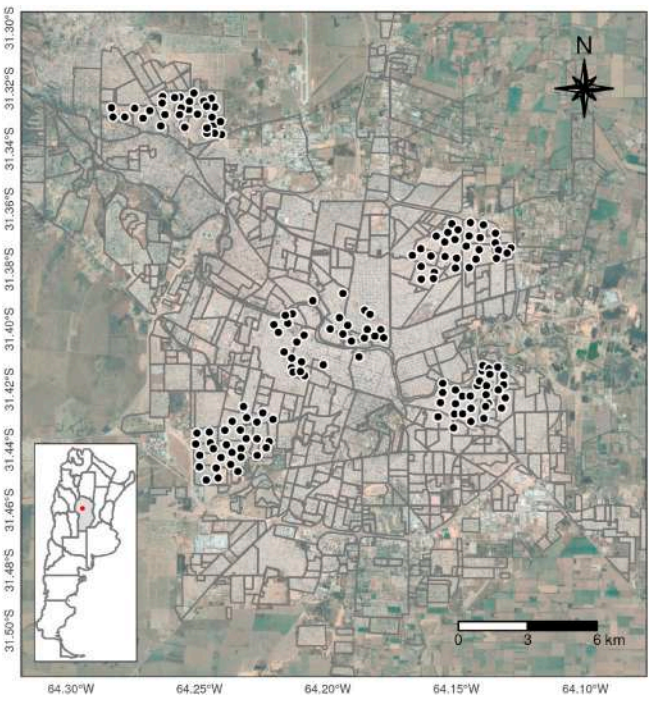

Fig. 1. Distribution of ovitraps in Córdoba city (Argentina).

aegypti larvae or pupae were considered positive. All entomological samples were collected and processed by the Zoonosis Division of the Health Ministry of Córdoba province (Argentina).

2.2.2. Satellite imagery and geospatial data

We used three Satellite Pour l'Observation de la Terre (SPOT) scenes covering Córdoba city. The images corresponded to: November 5, 2017 (SPOT 6); December 14, 2017 (SPOT 7) and March 15, 2018 (SPOT 6). The dates selected depended on availability, cloud coverage and mosquito reproductive season. SPOT 6 and 7 imagery consists of four bands (three visible and one near infra red) with 6 m of spatial resolution. Images were provided by the Argentinian Space Agency (CONAE, https://catalogos.conae.gov.ar/catalogo/catalogoSat.html) given an agreement with the French Space Agency (CNES, https://cnes.fr/en).

We also obtained geospatial data corresponding to neighbourhoods, railways, rivers and channels in Córdoba city from the state dataset available online (https://datosestadistica.cba.gov.ar/dataset/ciudad-de-cordoba).

2.3. Data processing

A diagram of the full workflow implemented in this study is presented in Fig. 2 and the scripts developed are available in a public repository (https://github.com/veroandreo/aedes-urban-maps). After atmospheric correction, common vegetation and water indices such as the Normalized Difference Vegetation Index (NDVI) and the Normalized Difference Water Index (NDWI) were derived from SPOT imagery, along with different texture measures (e.g., entropy, contrast, correlation) as to get synthetic bands for further steps in image analysis. Texture measures might be extracted from spectral bands or indices. In this case, we estimated the aforementioned texture measures from the near-infrared band given its known association with vegetation. A *k-means* unsupervised classification with 15 different classes was performed in order to identify different spectral covers over the city, following a methodology similar to that used by (Espinosa et al., 2016a). Once we obtained the classified map, we estimated distance to each of the identified classes. The results of the unsupervised classifications are presented in Fig. S2 in the Supplementary Material.

A buffer of 100 m radio surrounding each ovitrap was overlaid upon all synthetic bands and different statistics were obtained, i.e., number of classes, the most common class, class diversity indices, NDVI and NDWI mean and standard deviation, interspersion, etc. The full list of initially estimated variables with their respective description is presented in Table S1 of the Supplementary Material. The size of the buffer was established according to the average flight range of host seeking females mosquitoes (Reiter et al., 1995).

We also estimated distance to rivers, channels and railways. Our assumption was that these areas and their surroundings might represent suitable conditions for mosquitoes, acting as a source of adults. Therefore, the closer the ovitrap was to the river or a channel, the higher the chances of showing oviposition activity. All remote sensing and GIS processing was done in GRASS GIS 7.8 (GRASS Development Team, 2019).

The selection of environmental layers was based on availability known and *a priori* expectation of influences over the mosquito population (Espinosa et al., 2016b; Rotela et al., 2017; Rojas et al., 2017; Albrieu-Llinás et al., 2018; Estallo et al., 2018; Chen et al., 2019). We did not include aspect, temperature or precipitation because their spatial

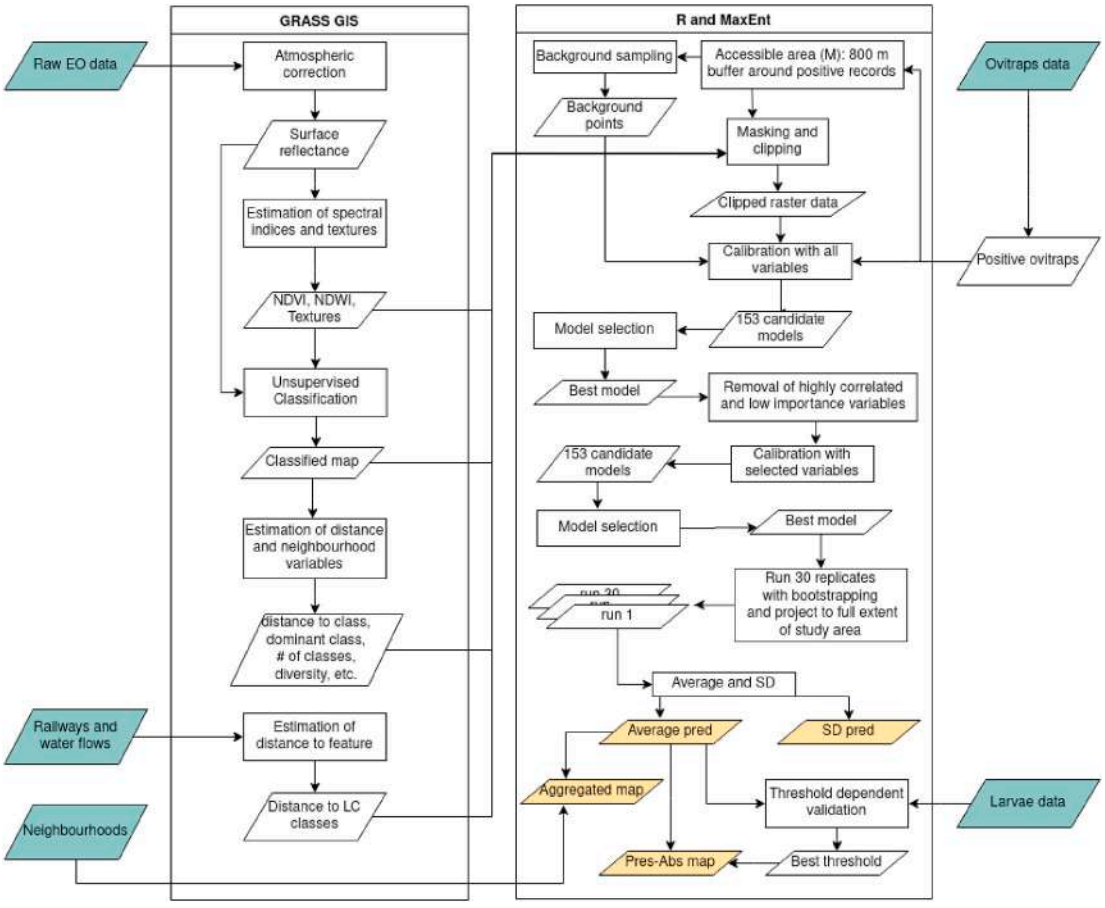

Fig. 2. Schematic representation of the workflow implemented. Aquamarine parallelograms are the input data, while yellow ones represent the different outputs obtained. (For interpretation of the references to colour in this figure legend, the reader is referred to the Web version of this article.)

resolution is (much) coarser than the resolution of SPOT imagery and downscaling of such variables was out of the scope of this study.

2.4. Modeling and analysis

We used MaxEnt 3.4.1 to model the distribution of *Ae. aegypti* and generate potential distribution maps (Phillips et al., 2017). MaxEnt is a machine-learning method that estimates the species potential geographic distribution by finding the probability distribution of maximum entropy (closest to uniform), subject to the constraint of the expected values of the environmental predictors (Phillips et al., 2006). MaxEnt was developed for presence-only data by contrasting presences against background locations (Phillips et al., 2006; Merow et al., 2013), and has shown to outperform other algorithms, even when used with few positive records as in our case (Elith et al., 2006; Hernandez et al., 2006; van Proosdij et al., 2016).

The ovitraps that evinced oviposition activity were considered positive, and thus used as presence sites in modeling procedures. For each of the dates studied, we used the positive ovitraps in a period of three weeks around the dates of the satellite imagery (November 2017: weeks 44–46; December 2017: weeks 49–51; March 2018: weeks 10–12) as presence records. To minimize sampling bias and the impact of assumptions about absences from areas that are not accessible to the species (Barve et al., 2011), we restricted model calibration (and thus background sampling) to the area where the species more likely had access to via dispersal. We defined this accessible area (M, Soberon and Peterson 2005) as the area within 800 m radio of each presence record. We chose this distance based on the maximum dispersal distance observed by Honório et al. (2003) for *Ae. aegypti* females in Rio de Janeiro. Background sampling was set to 10,000 points as in default settings.

The complexity of models built with MaxEnt can be adjusted with the inclusion of additional feature classes (i.e., transformations of the original predictor variables), as well as with a regularization multiplier that contributes to select those features and to reduce over-fitting (Merow et al., 2013). To determine the optimal model complexity, we calibrated preliminary models for the three selected months within the 2017–2018 mosquito season using the *kuenm* R package (Cobos et al., 2019) and including all the variables derived from remote sensing described above (Section 2.3). We explored all combinations of: a) 17 values of the regularization multiplier (0.1–1.0 by steps of 0.1, 2–6 by steps of 1, and 8 and 10), and b) nine sets of potential combinations of the four feature classes available: linear "l", quadratic "q", product "p", and hinge "h" (l, lq, lp, lqp, h, lh, lqh, lph, lqph). A total of 153 candidate preliminary models were calibrated for each of the months studied, and each model was evaluated according to statistical significance (partial ROC tests), performance (omission rate), and the Akaike's Information Criterion corrected for small sample sizes (AICc) (Cobos et al., 2019). The best preliminary model for each month was selected following the three criteria mentioned above: first, statistical significance <0.05; then omission rate $<5\%$; and finally $\Delta AICc < 2$ (Cobos et al., 2019).

After determining the optimal parameters of each preliminary model, we reduced model complexity by performing variable selection. We applied two procedures available in the *SDMtune* R package (Vignali et al., 2019, 2020): removal of highly correlated variables ($r > 0.7$), followed of removal of variables with low contribution/importance for model performance (percent contribution $< 5\%$).

Once we obtained the sets of relevant variables for each date, we conducted a detailed model selection exercise, exploring once again, all combinations of the 17 values of the regularization parameter and the nine combinations of the four feature classes (see above). Again, a total of 153 candidate models were calibrated for each date, now only including the uncorrelated and most relevant variables. These models were evaluated and selected as detailed above, i.e., statistical significance, omission rate and ΔAICc.

After determining the best parameter settings for each date, we ran 30 bootstrap replicates (500 iterations each), with extrapolation and clamping, and retaining a random partition of 25% of the points from each run (i.e., models were trained with a different 75% of data in each run). These final models, though only calibrated across M, were transferred to the full extent of the study area. We used the "cloglog" (Phillips et al., 2017) output format to assess average values across replicates as an estimate of the spatial distribution of suitable and unsuitable conditions for the oviposition of *Ae. aegypti*. The uncertainty in model predictions was assessed using the standard deviation in the suitability values across the model replicates. We assessed the overall discrimination ability of each model on the basis of the area under the receiver operating characteristic (ROC) curve (AUC).

We then extracted the average of the cloglog output per neighbourhood. In this way, we intended to visualize the spatial and temporal variability of suitability also in an aggregated manner according to meaningful spatial units in terms of monitoring and implementation of prevention and control plans.

2.5. Validation

We used presence/absence data derived from monthly larvae surveys to perform a threshold dependent validation of final models. Particularly, to validate the predictive map of each of the dates considered, we used larvae data from the subsequent month, e.g., to validate November 2017 model output we used larvae surveys from December 2017. Table 1 shows the number of positive records used for training and the number of positive and negative larval records used in validation.

For each date, we extracted the predicted probability for the pixel beneath the presence or absence coordinates plus the four neighbouring pixels. With this, we intended to minimize potential localization and projection errors.

We estimated presence/absence thresholds according to different well-known criteria (Liu et al., 2005, 2013): minimum occurrence prediction, mean occurrence prediction, 10% omission, sensitivity = specificity, maximum sensitivity + specificity, maximum proportion of presence and absence records correctly identified and minimum ROC (plot distance; the threshold value or range of values where the ROC curve is closest to point 0,1). For each threshold, we obtained a confusion matrix that allowed us to estimate different model accuracy metrics (Table 2, Liu et al., 2005). The threshold-dependent validation was performed with the package, SDMTools (VanDerWal et al., 2019) in R 3.6 (R Core Team, 2019).

3. Results

The final MaxEnt models obtained after variable selection and final calibration are shown in Fig. 3. The predicted average suitability for *Ae. aegypti* is generally high in the urbanized area of Córdoba city and low or very low in the city outskirts and rural surroundings, respectively. This pattern was pretty constant in all three months studied. There were also some low predicted probabilities in the core commercial area in the city center, as well as very low probabilities in large vegetated areas such as "Parque Sarmiento", a big park located in between southeast and southwest groups of ovitraps (Figs. 1 and 3).

Table 3 shows the best hyper-parameter settings (i.e., best

Table 1
Number of presence and absence records from ovitraps and larvae surveys in each period selected. For training, only presence records from ovitraps were used. For validation, records were derived from larvae surveys.

	Ovitraps			Larval surveys	
Date	pres	abs	Date	pres	abs
Nov 2017	38	112	Dec 2017	48	25
Dec 2017	134	16	Jan 2018	115	33
Mar 2018	146	4	Apr 2018	17	52

Table 2
Threshold-dependent measures used for assessing the predictive performance of models. References: TP, the number of presence points correctly classified as present; TN, the number of absence points correctly classified as absent; FP, the number of actual absence points classified as present; FN, the number of actual presence points classified as absent; P, the total number of actual presences; N, the total number of actual absences.

Performance measure	Definition	Formula
Sensitivity	True presences correctly predicted	TP/P
Specificity	True absences correctly predicted	TN/N
False positive rate		FP/N
False negative rate		FN/P
Positive predictive value	Predicted presences that were real	TP/(TP + FP)
Negative predictive value	Predicted absences that were real	TN/(TN + FN)
Overall Accuracy	Proportion of presences and absences correctly predicted	TN + TP/(P + N)

combination of regularization multiplier and feature classes) resulting from calibration after variable selection for each period studied. All models were highly significant, presented omission rates below 5% and had the lowest AICc values (See Table S2 in the Supplementary Material for a summary of the first ten models obtained for each date).

From the ROC figures (Fig. 4) and according to AUC values, the predictive performance of final models (based on the training data set) was average in general. Sensitivity and specificity were obtained for the threshold where sensitivity + specificity is maximal. In general, models seemed to be more sensible than specific (i.e., they where better in predicting positive than negative sites). However, the negative predictive value was very high for all three months opposite to the positive predictive value that was very low.

The variables that were retained as best predictors for each month with their respective contribution and importance are shown in Table 4. Most important variables varied for different dates. Only the variable *distance to class 14* appeared as an important predictor in all cases. Class 14 is representing borders of buildings and some asphalted surfaces (See detail in the Supplementary Material). The most important variable, in terms of contribution and importance, was correlation, both in December 2017 and March 2018 (Table 4). This variable was obtained from the near infrared (NIR) band and represents the correlation among grey levels in 100 m radio areas. There were some other variables that appeared to be important in two out of the three final models: distance to class 2 (represented by green crops and vegetated areas, see detail in Fig. S4 in the Supplementary material), distance to the railway and correlation estimated over the NIR band.

The distance to buildings (class 14) presented a negative relationship with suitability in the three periods studied. However, the shape and steepness of the curve varied slightly (Fig. 5). The distance to vegetated surfaces (class 2) showed different response curves in November and March (Fig. 5a and c), the same than distance to railway that appeared to have a different response in December and March (Fig. 5b and c).

The performance of models as evaluated with larvae survey data and threshold dependent metrics was rather poor, with maximum overall accuracy of 0.78 (Table 5). Sensitivity appeared high in many cases but the counterpart, specificity, was very low, which means that models performed much better in predicting presences than absences. This was also evident in positive and negative predictive values (PPV and NPV, Table 5). These results made it difficult to select a threshold better than the arbitrary 0.5 to classify the predicted suitability into presence and absence.

Since threshold dependent validation did not yield a clear best threshold value (Table 5), we used a fixed probability of 0.5 to classify maps in presence and absence. From that, we obtained that ≈42% of the city surface can be classified as presence in November, 85% in December and ≈45% in March. In order to better visualize which areas increase or decrease their suitability, we used the binary maps described above to create difference maps as follows: December–November and March–December. We observed that the areas becoming more suitable from November to December are different from those becoming more suitable from December to March (Fig. 6). In the first case, peripheral areas increase their suitability, while in the second, these areas seem to decrease their suitability in favor of more central parts of the city.

After estimating the average probability per neighbourhood in each period studied, we can observe how suitability changes as season proceeds, with the highest probabilities covering larger parts of the city in December (Fig. 7, central panel). Some neighbourhoods, on the other hand, remain with low probabilities most of the season. These are, however, neighbourhoods with a low proportion of urbanized land (see for example those in the north or in the south and compare with Fig. 1). In general, the aggregated maps reflect the same pattern than the difference maps in Fig. 6. In this case, however, the percentages of the city surface with suitability higher than 0.5 are: 38, 55 and 38 for November, December and March, respectively.

4. Discussion

This work presents an approach that reinforces operational procedures of public health authorities based on a scientific method, integrating spatial analysis, EO data and data of presence and absence of the vector in an urban area of significant extension. The workflow allows to obtain predictive maps for *Ae. aegypti* oviposition suitability (Fig. 2). Instead of aggregating mosquito data to build a unique map, we modelled and mapped monthly oviposition for three different months within *Ae. aegypti*'s activity period according to the availability of EO data to examine the spatial changes in suitability as the mosquito season proceeds.

We found that both distance to build-up surfaces (class 14) and correlation (a proxy of surface homogeneity, where high values indicate an homogeneous area within a 100 m radio) were important predictors of habitat suitability for oviposition (Table 4) and they showed a negative relationship in the response curves (Fig. 5). Consequently, the urbanized areas showed much higher probabilities than the rural areas. Moreover, the vegetated areas within the city as well as the core commercial downtown showed low (er) suitability (Fig. 3). These spatial patterns within urban areas (positive association with neighbourhoods, but negative with vegetated and large concrete areas) are well known for *Ae. aegypti* (Tsuda et al., 2006; Rey et al., 2007; Khatchikian et al., 2011; Espinosa et al., 2016a,b) and they have been related to the availability of human blood-meal sources as well as the provision of artificial water-holding containers in and around human dwellings (Carbajo et al., 2006; Powell and Tabachnick, 2013; Cardo et al., 2014; Heinisch et al., 2019).

Correlation values around 0.5–0.6 showed the highest suitability for oviposition (Fig. 5). In a 100 m radio then, female mosquitoes seem to prefer areas with intermediate values of correlation, i.e., not so homogeneous. This could explain the low suitability of the core commercial center and large vegetated areas within the city, as well as the rural surroundings, where correlation in a 100 m radio was much higher, i.e., the area within that distance is more homogeneous. The importance of landscape factors for mosquito abundance was already observed by Chen et al. (2019). Indeed, more heterogeneous environments, where the proportion of houses (instead of high buildings) is high (Carbajo et al., 2006), might offer the proper combination of temperature, humidity, shadowed areas (i.e., vegetated backyards) and containers' availability that favor oviposition and further larval development (Vanwambeke et al., 2007).

Distance to crops and vegetated surfaces (class 2) was also a relevant predictor of habitat suitability for oviposition according to importance values (Table 4). The shape of the response curve was different in November and March, but there seems to be an optimum distance around 150 m from which the suitability decays either steeply or very

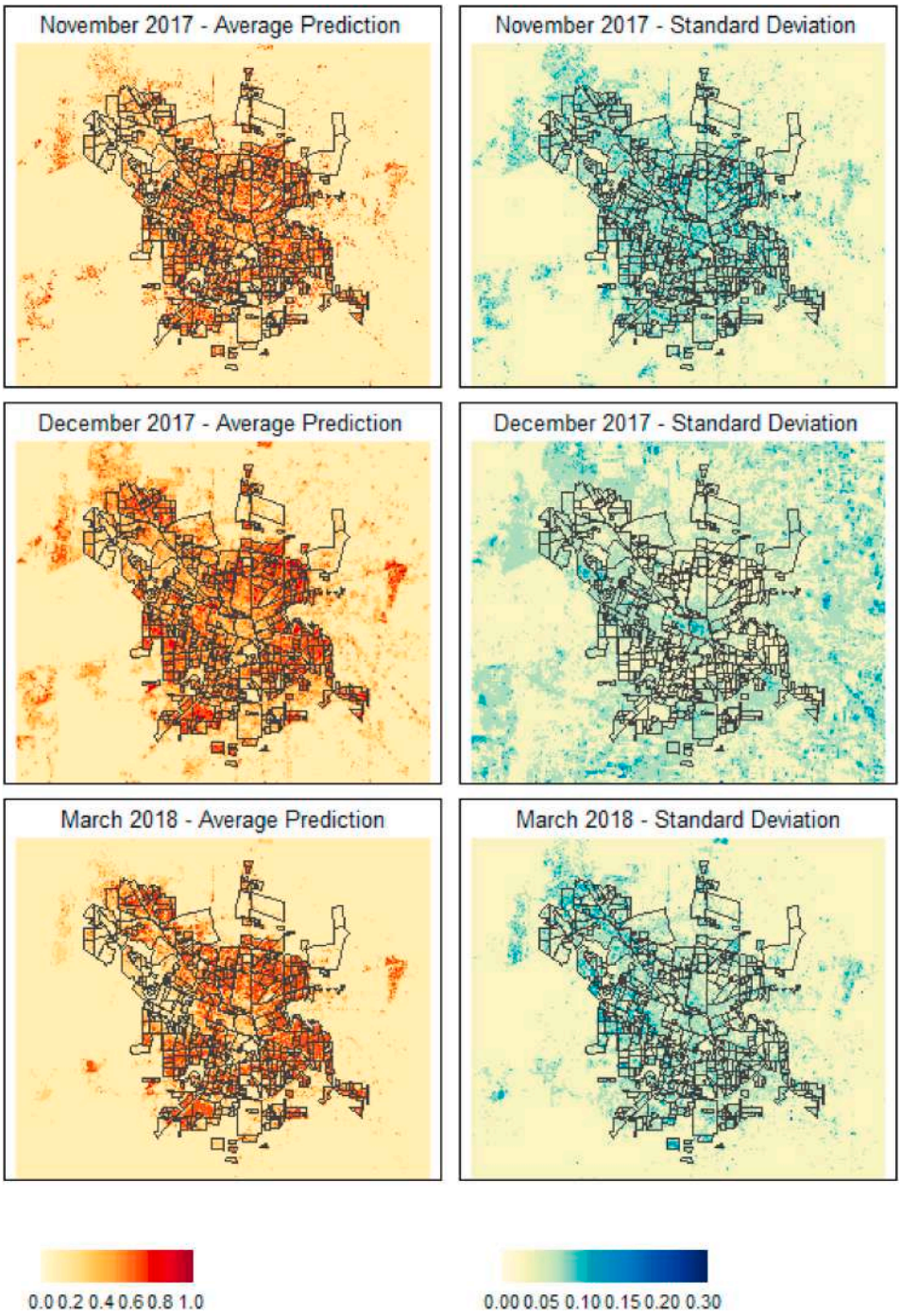

Fig. 3. Average predicted suitability for *Ae. aegypti* in Córdoba city and corresponding standard deviation.

Table 3
Performance metrics for parameter settings regarding regularization multiplier (RM) and feature classes (FC) used for creating final models. FCs are as follows: linear = l, quadratic = q, product = p, and hinge = h.

Date	RM	FC	Partial ROC	Omission rate 5%	AICc	ΔAICc	AICc weights
Nov 2017	0.5	lqp	0.00	0.00	1047.7	0.00	0.30
Dec 2017	6	l	0.00	0.03	3827.46	0.00	0.99
Mar 2018	3	h	0.00	0.00	4157.41	0.00	0.29

slowly (Fig. 5). This might be explained by female mosquitoes' (mean) flight range and the availability of shadowed places were to lay eggs or rest. Associations with vegetation cover as measured by NDVI were already observed in Córdoba city (Estallo et al., 2018) and elsewhere (Ostfeld et al., 2005; Philbert and Ijumba, 2013).

Within the urbanized area, suitability varied during the season (Fig. 6) consistently with previous studies that showed a seasonal pattern of increased suitability in December and January decreasing

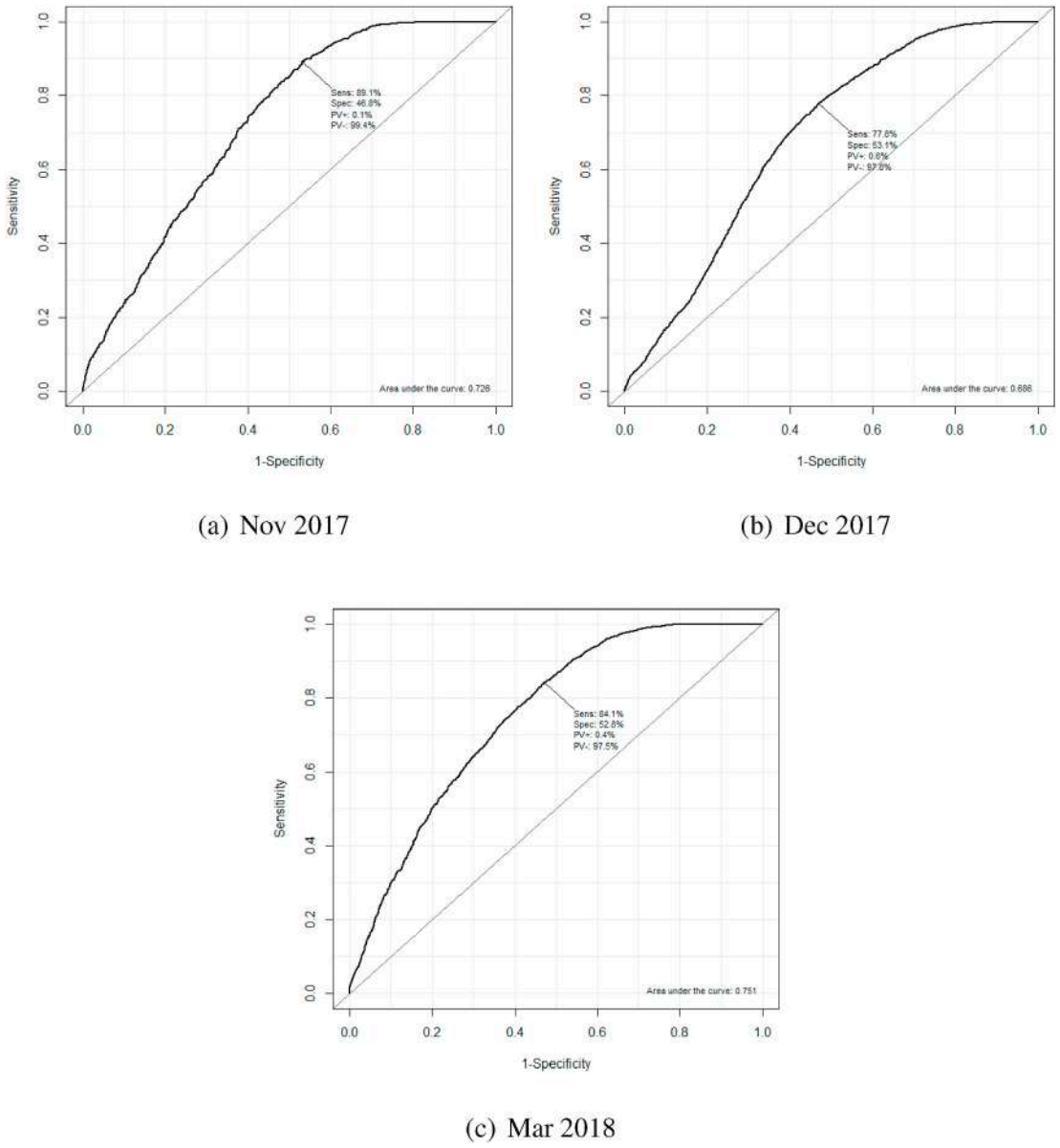

Fig. 4. Receiver-operator curves (ROC) for final MaxEnt models. References: AUC, area under the receiver-operator curve; Sens, sensitivity; Spec, specificity; PV+, positive predictive value; PV-, negative predictive value.

towards March (Rojas et al., 2017). The predictive maps obtained are also roughly consistent with studies analyzing oviposition (Dominguez et al., 2000; Andreo et al., 2019; Porcasi et al., 2019) and mosquito abundance (Gleiser and Zalazar, 2010) in Córdoba city. These have found high oviposition in the southeastern part of the city where suitability values were generally high (Figs. 3 and 7). This area is mostly residential, though there are parts that hold informal settlements. The cemetery of the city is located in the south eastern part of the city, too. The combination of these conditions might create a higher proportion of potential breeding sites for female mosquitoes. Cemeteries have already been described as highly suitable areas for container-breeding mosquitoes (Vezzani, 2007).

The evaluation metrics obtained from models' calibration (Fig. 4) yielded values coinciding with an average predictive performance (i.e., AUC between 0.7 and 0.8, Araújo and Guisan, 2006). The validation with independent data, larvae surveys carried out in different parts of the city (see Supplementary Material), provided poor results (Table 5). The validation measures obtained (mainly specificity) might be influenced by the fact that the independent data used refers to a different mosquito life stage (i.e., with potentially different habitat requirements). However, the observed hatching rate for eggs of *Ae. aegypti* in Córdoba city is 93% (Dominguez et al., 2000). Hence, we think that the main factor affecting the results of validation with independent data is related moreover to the clustered distribution of ovitraps. To account for this sample bias, both background sampling and model calibration were performed in an area of 800 m radio from positive sites (See section 2.4). Still, it could be explaining the high sensitivity and the low specificity values that we observed in general (Table 5), i.e., models are good in identifying highly suitable areas but fail to identify/predict low suitability sites. In any case, in applications related to human health, sensitivity is usually more relevant than specificity, i.e., we want to know where mosquito might develop even if some areas might be false positives. Importantly, despite the validation measures were not as good as we expected, they do not undermine the proposed method. Indeed, the problem might be arising from the clustered distribution of ovitraps and future applications and monitoring designs should take this into account.

The spatial resolution of EO data used might have also influenced our

Table 4
Variable importance: percent contribution and permutation importance (average and standard deviation).

Date	Variable	Percent Contribution	Permutation Importance
Nov 2017	Distance to Class 2	20.73 (11.80)	32.75 (14.19)
	Distance to Class 13	27.93 (23.14)	44.35 (15.50)
	Distance to Class 14	48.63 (21.48)	19.93 (13.05)
Dec 2017	Distance to Railway	0.54 (2.06)	0.03 (2.49)
	Distance to Class 14	31.19 (9.63)	12.91 (10.67)
	NDWI Average	4.48 (6.31)	17.05 (11.21)
	Correlation	49.77 (10.75)	36.70 (13.23)
	Contrast	12.71 (7.72)	30.53 (11.59)
Mar 2018	Distance to Railway	7.69 (3.77)	14.34 (6.08)
	Distance to Class 2	32.71 (12.81)	17.41 (12.47)
	Distance to Class 10	2.29 (4.14)	11.30 (7.07)
	Distance to Class 14	13.13 (10.91)	16.34 (9.27)
	Correlation	36.20 (10.50)	33.99 (9.13)

results, as well as the size of the buffer we used. Further studies should address different buffer sizes since literature is variable regarding mean and maximum flight distance of *Ae. aegypti* females (Honório et al., 2003; Verdonschot and Besse-Lototskaya, 2014). Most previous studies have used EO data with spatial resolutions equal to or higher than 6 m (Carbajo et al., 2006; Arboleda et al., 2012; Estallo et al., 2018). This prevents the identification of smaller features and potential associations with mosquitoes activity. Higher resolution EO data (less than 5 m) which would provide more detailed environmental information is not freely available and hence, not affordable for a monthly operative product as the one we propose.

In our analysis, we could not identify an optimal threshold value with the threshold dependent validation. However, several criteria were around 0.5. Therefore, we used this arbitrary value to be able to represent binary maps and visualize suitability changes as the difference between monthly maps (Fig. 6). From November to December we observed that suitable surface increases and then it diminishes towards March. This pattern is consistent with seasonal oviposition curves (Dominguez et al., 2000; Andreo et al., 2019) and changes observed in entomological indices (Rojas et al., 2017). The areas that became more suitable from November to December are mostly characterized by residential neighbourhoods, that might offer the heterogeneity needed for mosquitoes to meet their habitat requirements (Carbajo et al., 2006). Towards March many areas became unsuitable, while others increased their suitability. Notably most of the northwestern part of the city remained unchanged (Fig. 6). It is difficult to explain these later changes without maps for the intermediate months. However, we can think of structural differences among neighbourhoods in terms of proportions of different classes and their spatial configuration, which could provide more suitable habitat for oviposition in different moments of the season. There can also be other explanatory factors that were not considered here. Estallo et al. (2018), for example, included socioeconomic and other urban land use related variables that resulted important in their predictive model. However, such variables are usually outdated (e.g., the last population census data available is from 2010) or do not have the spatial resolution required for a detailed map.

To favor rapid response by public health authorities, we aggregated suitability values over neighbourhoods (Fig. 7). These aggregated maps could provide a quicker indication of where and when to concentrate efforts given the limited human and monetary resources assigned to prevention and control measures. In this context, despite some disadvantages, ovitraps are a useful and low-cost method for detecting and monitoring *Ae. aegypti*, mainly when adult densities are low (Focks and Diseases, 2004; Barrera et al., 2019). Indeed, they become highly relevant to model and predict habitat suitability at the beginning and end of the season, which coincides with higher AUC values (Fig. 4). Since mosquito biology and disease ecology are strongly linked to environmental conditions, the prediction of *Ae. aegypti* presence/activity at the beginning of the warm season in temperate climates might be key for the preparedness for a rapid response.

In this contribution, we aimed at obtaining not only the mosquito predictive maps, but especially an operative workflow (Porcasi et al., 2012) requiring minimum human intervention. Indeed, we implemented a chain (Fig. 2) that builds upon long standing free and open source software such as GRASS GIS (GRASS Development Team, 2019), R (R Core Team, 2019) and MaxEnt (Phillips et al., 2017). This ensures its the reproducibility usability of the method since the tools are freely available. Importantly, we propose a workflow *towards* an operational system that includes data input, processing, modeling, validation and output. The steps in this workflow can be re-used for other cities and input EO data by only adapting window sizes according to spatial resolution and, either specifying proper atmospheric correction parameters or removing this step by using already corrected products, such as Sentinel 2 level 2 A or Landsat 8. Even though we implemented our proof of concept workflow using manually selected SPOT imagery, we are inclined to switch to Sentinel 2 data to make the chain fully reproducible (Frery et al., 2020). Furthermore, the revisit time of Sentinel 2 would allow for more images within a given period (eg., one month) in case of cloudy scenes. This would also allow for temporal aggregation of scenes instead of relying on a single image. Furthermore, it can be easily adapted to intake other EO data sources like ESA Sentinel 2 satellite with a spatial resolution of 10 m. The workflow can also be adapted to use a supervised approach if labeled cover classes are desired. In any case, unsupervised classes have denoted consistency across months and indeed, the same classes appeared as important predictors either in the three, or two out of the three moments studied (Table 4). On the side of mosquito data, we are collaborating with health authorities to make the upload and download of ovitraps and larvae data a more fluent process.

5. Conclusion

While EO data availability has increased dramatically in the last decade, their use in operational systems with social impact is still very limited. Filling this gap constitutes a huge challenge for the space agencies and the geo-science and remote sensing academic community. With this in mind, we presented here an operative workflow towards an operative system to obtain *Ae. aegypti* suitability maps. It requires minimum intervention and can be further automated, and adapted to other EO data. This workflow was carefully thought as to consider possible biases in training data, calibration of many models to obtain the optimum hyper-parameters combination, model selection, variable selection and validation.

In general, we found high suitability within the city, except in large vegetated areas and the commercial downtown. These results were consistent with previous studies and our own observations in the field. The maps confirmed the need to maintain the monitoring activities that are carried out so far (ovitraps and larvae surveys). Our results did suggest, however, that the present distribution of ovitraps might affect the predictive performance of models. A more random or systematic distribution across the city would be desirable.

All the steps in our process chain were implemented using freely available and open source software. This warrants the possibility to reuse and modify the method since there is no proprietary licences involved. Moreover, it allows for changes in terms of methods or according to available EO and mosquito data. Finally, it is important to remark that although our workflow does not constitute (yet) a fully operational system that can be replicated without modification, we

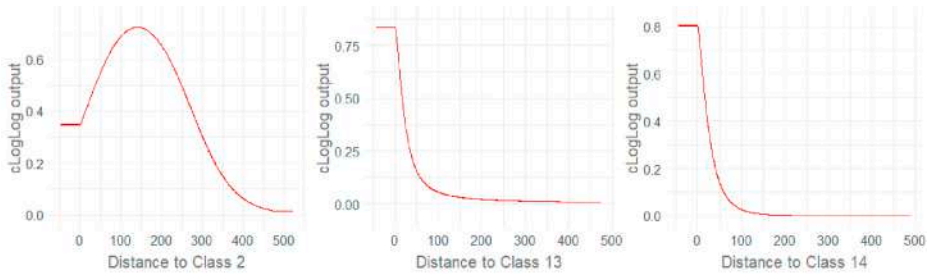

(a) Nov 2017

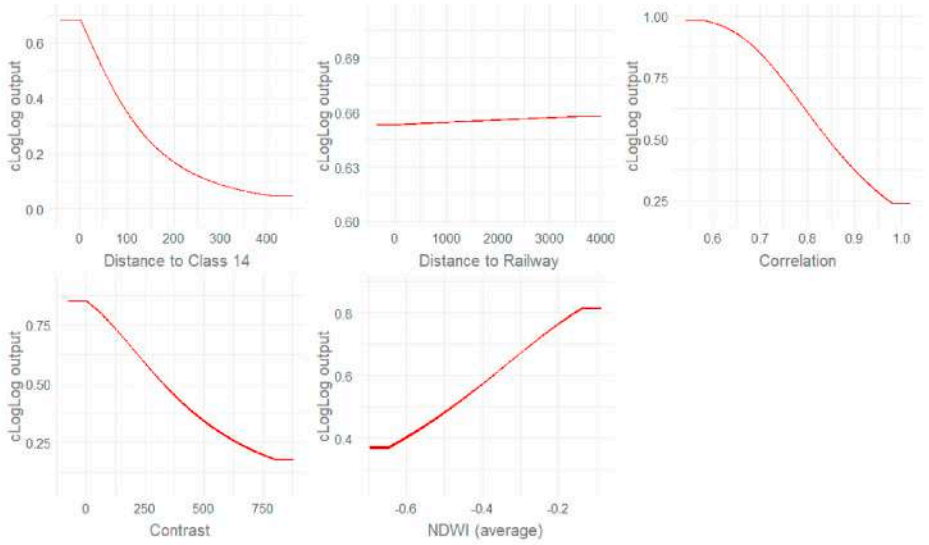

(b) Dec 2017

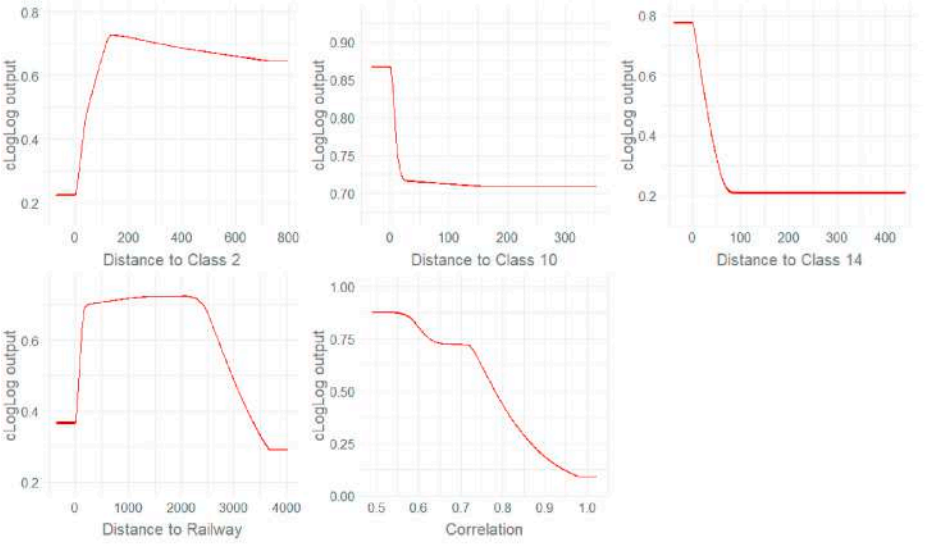

(c) Mar 2018

Fig. 5. Response curves for variables retained in November 2017 (top), December 2017 (center) and, March 2018 (bottom) models.

Table 5
Evaluation of models' performance using different criteria for threshold selection. Evaluation was carried out with larvae surveys belonging to the corresponding following month to that being modelled. References: roc, receiver operator curve; FPR, false positive rate; FNR, false negative rate, NPV, negative predictive value; OA, overall accuracy.

Month	Criteria	Thres	Sens	Spec	FPR	FNR	PPV	NPV	OA
Nov 2017	min.occ.pred	0.115	1.000	0.000	1.000	0.000	0.658	nan	0.658
	mean.occ.pred	0.531	0.521	0.680	0.320	0.479	0.758	0.425	0.575
	10.perc.omis	0.320	0.896	0.200	0.800	0.104	0.683	0.500	0.658
	sens = spec	0.480	0.646	0.640	0.360	0.354	0.775	0.485	0.644
	max.sens + spec	0.490	0.625	0.680	0.320	0.375	0.789	0.486	0.644
	max.prop.cor	0.390	0.792	0.400	0.600	0.208	0.717	0.500	0.658
	min.ROC.dist	0.490	0.625	0.680	0.320	0.375	0.789	0.486	0.644
Dec 2017	min.occ.pred	0.263	1.000	0.000	1.000	0.000	0.777	nan	0.777
	mean.occ.pred	0.604	0.565	0.606	0.394	0.435	0.833	0.286	0.574
	10.perc.omis	0.42	0.904	0.121	0.879	0.096	0.782	0.267	0.730
	sens = spec	0.590	0.609	0.606	0.394	0.391	0.843	0.308	0.608
	max.sens + spec	0.590	0.609	0.606	0.394	0.391	0.843	0.308	0.608
	max.prop.cor	0.26	1.000	0.000	1.000	0.000	0.777	nan	0.777
	min.ROC.dist	0.590	0.609	0.606	0.394	0.391	0.843	0.308	0.608
Mar 2018	min.occ.pred	0.116	1.000	0.000	1.000	0.000	0.754	nan	0.754
	mean.occ.pred	0.591	0.596	0.294	0.706	0.404	0.721	0.192	0.522
	10.perc.omis	0.280	0.904	0.059	0.941	0.096	0.746	0.167	0.696
	sens = spec	0.650	0.481	0.529	0.471	0.519	0.758	0.250	0.493
	max.sens + spec	0.760	0.173	1.000	0.000	0.827	1.000	0.283	0.377
	max.prop.cor	0.170	0.981	0.059	0.941	0.019	0.761	0.500	0.754
	min.ROC.dist	0.680	0.404	0.647	0.353	0.596	0.778	0.262	0.464

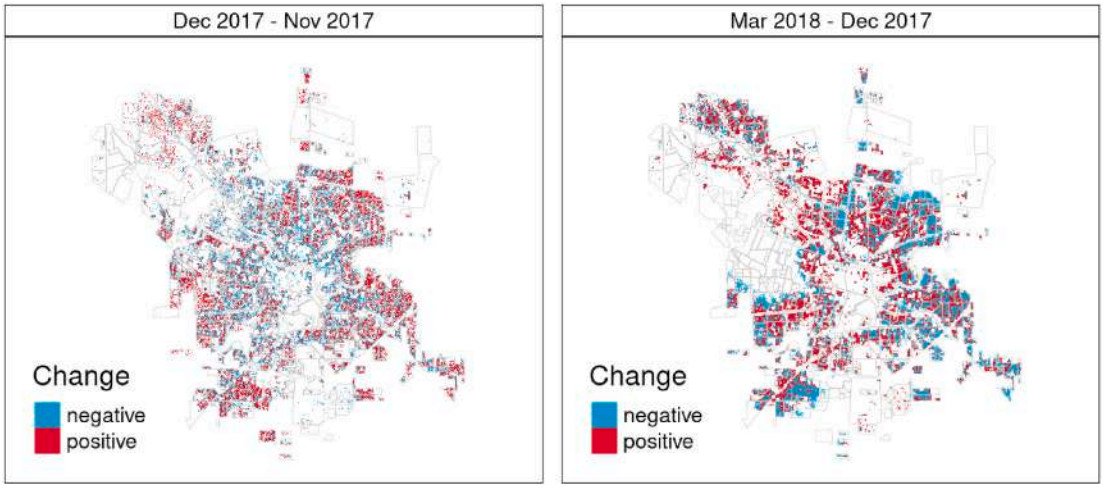

Fig. 6. Positive and negative changes in suitability from November to December and December to March in Córdoba city (Argentina). Before estimating the difference, predictive maps were converted to presence/absence with a threshold of 0.5. Changes are hence estimated only for probabilities of presence.

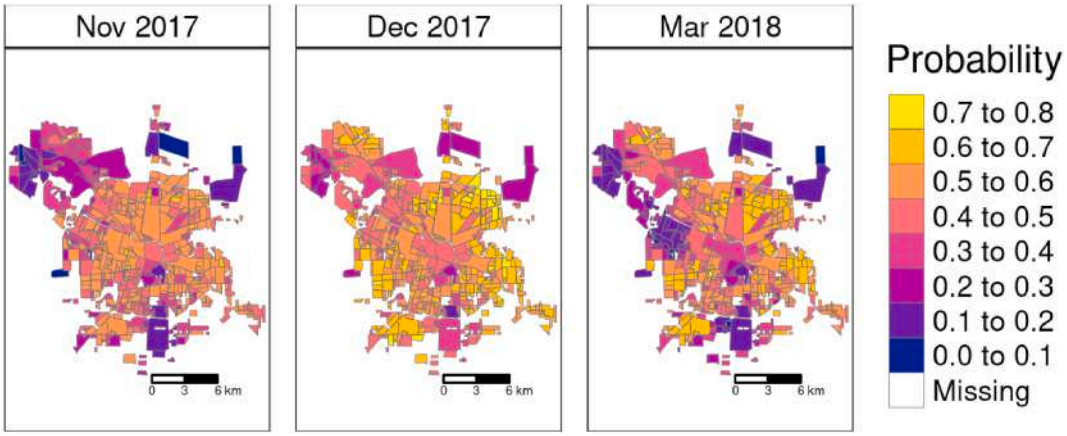

Fig. 7. Average suitability aggregated by neighbourhoods in Córdoba city (Argentina).

consider it is an important contribution in terms of tools and procedures in that direction.

Funding

This research did not receive any specific grant from funding agencies in the public, commercial, or not-for-profit sectors.

Author contributions

VA and PFC designed the study, VA processed the EO data, PFC performed the modeling, VA and PFC analyzed the results, VA led the writing of the manuscript with contributions from PFC, all the authors revised and agreed to the final version.

Declaration of competing interest

The authors declare that they have no known competing financial interests or personal relationships that could have appeared to influence the work reported in this paper.

Acknowledgements

The authors would like to thank the Argentinean Space Agency (CONAE, https://www.argentina.gob.ar/ciencia/conae) for the SPOT imagery and the Health Ministry of Córdoba province for the mosquito data.

Appendix A. Supplementary data

Supplementary data to this article can be found online at https://doi.org/10.1016/j.rsase.2021.100554.

References

Albrieu-Llinás, G., Espinosa, M.O., Quaglia, A., Abril, M., Scavuzzo, C.M., 2018. Urban environmental clustering to assess the spatial dynamics of *Aedes aegypti* breeding sites. Geospatial Health 13, 135–142. https://doi.org/10.4081/gh.2018.654.

Andreo, V., Porcasi, X., Rodriguez, C., Lopez, L., Guzman, C., Scavuzzo, C.M., 2019. Time series clustering applied to eco-epidemiology: the case of *Aedes aegypti* in córdoba, Argentina. In: 2019 XVIII Workshop on Information Processing and Control (RPIC), pp. 93–98. https://doi.org/10.1109/RPIC.2019.8882184.

Araújo, M.B., Guisan, A., 2006. Five (or so) challenges for species distribution modelling. J. Biogeogr. 33, 1677–1688. https://doi.org/10.1111/j.1365-2699.2006.01584.x.

Arboleda, S., Jaramillo, -O.N., Peterson, A.T., 2012. Spatial and temporal dynamics of *Aedes aegypti* larval sites in bello, Colombia. J. Vector Ecol. 37, 37–48. https://doi.org/10.1111/j.1948-7134.2012.00198.x.

Barbosa, G.L., Donalísio, M.R., Stephan, C., Lourenço, R.W., Andrade, V.R., Arduino, M. d.B., Lima, V.L.C.d., 2014. Spatial distribution of the risk of dengue and the entomological indicators in Sumaré, state of São Paulo, Brazil. PLoS Neglected Trop. Dis. 8, e2873 https://doi.org/10.1371/journal.pntd.0002873.

Barrera, R., Amador, M., Acevedo, V., Beltran, M., Muñoz, J.L., 2019. A comparison of mosquito densities, weather and infection rates of *Aedes aegypti* during the first epidemics of Chikungunya (2014) and Zika (2016) in areas with and without vector control in Puerto Rico. Med. Vet. Entomol. 33, 68–77. https://doi.org/10.1111/mve.12338.

Barve, N., Barve, V., Jiménez-Valverde, A., Lira-Noriega, A., Maher, S.P., Peterson, A.T., Soberón, J., Villalobos, F., 2011. The crucial role of the accessible area in ecological niche modeling and species distribution modeling. Ecol. Model. 222, 1810–1819. https://doi.org/10.1016/j.ecolmodel.2011.02.011.

Bhatt, S., Gething, P.W., Brady, O.J., Messina, J.P., Farlow, A.W., Moyes, C.L., Drake, J. M., Brownstein, J.S., Hoen, A.G., Sankoh, O., Myers, M.F., George, D.B., Jaenisch, T., Wint, G.R.W., Simmons, C.P., Scott, T.W., Farrar, J.J., Hay, S.I., 2013. The global distribution and burden of dengue. Nature 496, 504–507. https://doi.org/10.1038/nature12060.

Bowman, L.R., Donegan, S., McCall, P.J., 2016. Is dengue vector control deficient in effectiveness or evidence?: systematic review and meta-analysis. PLoS Neglected Trop. Dis. 10, e0004551 https://doi.org/10.1371/journal.pntd.0004551.

Carbajo, A.E., Curto, S.I., Schweigmann, N.J., 2006. Spatial distribution pattern of oviposition in the mosquito *Aedes aegypti* in relation to urbanization in Buenos Aires: southern fringe bionomics of an introduced vector. Med. Vet. Entomol. 20, 209–218. https://doi.org/10.1111/j.1365-2915.2006.00625.x.

Cardo, M.V., Vezzani, D., Rubio, A., Carbajo, A.E., 2014. Integrating demographic and meteorological data in urban ecology: a case study of container-breeding mosquitoes in temperate Argentina. Area 46, 18–26. https://doi.org/10.1111/area.12071.

Chen, S., Whiteman, A., Li, A., Rapp, T., Delmelle, E., Chen, G., Brown, C.L., Robinson, P., Coffman, M.J., Janies, D., Dulin, M., 2019. An operational machine learning approach to predict mosquito abundance based on socioeconomic and landscape patterns. Landsc. Ecol. https://doi.org/10.1007/s10980-019-00839-2.

Cheong, W.H., 1967. Preferred *Aedes aegypti* larval habitats in urban areas. Bull. World Health Organ. 36, 586–589.

Cobos, M.E., Peterson, A.T., Barve, N., Osorio-Olvera, L., 2019. kuenm: an r package for detailed development of ecological niche models using maxent. PeerJ 7, e6281. https://doi.org/10.7717/peerj.6281. https://peerj.com/articles/6281.

Cromwell, E.A., Stoddard, S.T., Barker, C.M., Rie, A.V., Messer, W.B., Meshnick, S.R., Morrison, A.C., Scott, T.W., 2017. The relationship between entomological indicators of *Aedes aegypti* abundance and dengue virus infection. PLoS Neglected Trop. Dis. 11, e0005429 https://doi.org/10.1371/journal.pntd.0005429.

Dominguez, M., Ludueña-Almeida, F., Almirón, W., 2000. Dinámica poblacional de *aedes aegypti* (Díptera: Culicidae) en Córdoba capital. Rev. Soc. Entomol. Argent. 59, 41–50.

Elith, J., Graham, H., C, P., Anderson, R., Dudík, M., Ferrier, S., Guisan, A., Hijmans, R.J., Huettmann, F., Leathwick, J.R., Lehmann, A., Li, J., Lohmann, G., Loiselle, L.A., B, Manion, G., Moritz, C., Nakamura, M., Nakazawa, Y., McC, M., Overton, J., Townsend Peterson, A., Phillips, S.J., Richardson, K., Scachetti-Pereira, R., Schapire, R.E., Soberón, J., Williams, S., Wisz, S., M, E., Zimmermann, N., 2006. Novel methods improve prediction of species' distributions from occurrence data. Ecography 29, 129–151. https://doi.org/10.1111/j.2006.0906-7590.04596.x.

Espinosa, M., Alvarez Di Fino, E.M., Abril, M., Lanfri, M., Periago, M.V., Scavuzzo, C.M., 2018. Operational satellite-based temporal modelling of *Aedes* population in Argentina. Geospatial Health 13. https://doi.org/10.4081/gh.2018.734.

Espinosa, M., Weinberg, D., Rotela, C.H., Polop, F., Abril, M., Scavuzzo, C.M., 2016a. Temporal dynamics and spatial patterns of *Aedes aegypti* breeding sites, in the context of a dengue control program in Tartagal (Salta province, Argentina). PLoS Neglected Trop. Dis. 10, e0004621 https://doi.org/10.1371/journal.pntd.0004621.

Espinosa, M.O., Polop, F., Rotela, C.H., Abril, M., Scavuzzo, C.M., 2016b. Spatial pattern evolution of *Aedes aegypti* breeding sites in an Argentinean city without a dengue vector control programme. Geospatial Health. https://doi.org/10.4081/gh.2016.471.

Estallo, E.L., Carbajo, A.E., Grech, M.G., Frías-Céspedes, M., López, L., Lanfri, M.A., Ludueña-Almeida, F.F., Almirón, W.R., 2014. Spatio-temporal dynamics of dengue 2009 outbreak in córdoba city, Argentina. Acta Trop. 136, 129–136. https://doi.org/10.1016/j.actatropica.2014.04.024.

Estallo, E.L., Sangermano, F., Grech, M., Ludueña-Almeida, F., Frías-Cespedes, M., Ainete, M., Almirón, W., Livdahl, T., 2018. Modelling the distribution of the vector *Aedes aegypti* in a central argentine city. Med. Vet. Entomol. https://doi.org/10.1111/mve.12323.

Focks, D.A., Diseases, U., 2004. A Review of Entomological Sampling Methods and Indicators for Dengue Vectors. World Health Organization. https://apps.who.int/iris/handle/10665/68575.

Frery, A.C., Gomez, L., Medeiros, A.C., 2020. A badging system for reproducibility and replicability in remote sensing research. IEEE Journal of Selected Topics in Applied Earth Observations and Remote Sensing 13, 4988–4995. https://doi.org/10.1109/JSTARS.2020.3019418.

Getis, A., Morrison, A.C., Gray, K., Scott, T.W., 2003. Characteristics of the spatial pattern of the dengue vector, *Aedes aegypti*, in Iquitos, Perú. Am. J. Trop. Med. Hyg. 12.

Gleiser, R., Zalazar, L., 2010. Distribution of mosquitoes in relation to urban landscape characteristics. Bull. Entomol. Res. 100, 153–158. https://doi.org/10.1017/S0007485309006919.

GRASS Development Team, 2019. Geographic resources analysis support system (GRASS GIS) software, version 7.8. Open Source Geospatial Foundation. https://grass.osgeo.org.

Gubler, D.J., 2011. Dengue, urbanization and globalization: the unholy trinity of the 21st century. Trop. Med. Health 39, 3–11. https://doi.org/10.2149/tmh.2011-S05.

Heinisch, M., Diaz-Quijano, F.A., Chiaravalloti-Neto, F., Menezes Pancetti, F.G., Rocha Coelho, R., dos Santos Andrade, P., Urbinatti, P.R., de Almeida, R.M.M.S., Lima-Camara, T.N., 2019. Seasonal and spatial distribution of *Aedes aegypti* and *Aedes albopictus* in a municipal urban park in São Paulo, SP, Brazil. Acta Trop. 189, 104–113. https://doi.org/10.1016/j.actatropica.2018.09.011.

Hernandez, P.A., Graham, C.H., Master, L.L., Albert, D.L., 2006. The effect of sample size and species characteristics on performance of different species distribution modeling methods. Ecography 29, 773–785. https://doi.org/10.1111/j.0906-7590.2006.04700.x.

Honório, N.A., Silva, W.d.C., Leite, P.J., Gonçalves, J.M., Lounibos, L.P., Lourenço-de Oliveira, R., 2003. Dispersal of *Aedes aegypti* and a*edes albopictus* (Diptera: Culicidae) in an urban endemic dengue area in the State of Rio de Janeiro, Brazil. Mem. Inst. Oswaldo Cruz 98, 191–198. https://doi.org/10.1590/S0074-02762003000200005.

INDEC, 2010. Censo nacional de Población, Hogares y Viviendas. Technical Report. Instituto Nacional de Estadística y Censo. http://www.censo2010.indec.gov.ar/preliminares/cuadrocordoba.asp.

Johnson, T.L., Haque, U., Monaghan, A.J., Eisen, L., Hahn, M.B., Hayden, M.H., Savage, H.M., McAllister, J., Mutebi, J.P., Eisen, R.J., 2017. Modeling the environmental suitability for *Aedes (Stegomyia) aegypti* and *Aedes (Stegomyia) albopictus* (Diptera: Culicidae) in the Contiguous United States. J. Med. Entomol. 54, 1605–1614. https://doi.org/10.1093/jme/tjx163.

Kalluri, S., Gilruth, P., Rogers, D., Szczur, M., 2007. Surveillance of arthropod vector-borne infectious diseases using remote sensing techniques: a review. PLoS Pathog. 3, e116 https://doi.org/10.1371/journal.ppat.0030116.

Khatchikian, C., Sangermano, F., Kendell, D., Livdahl, T., 2011. Evaluation of species distribution model algorithms for fine-scale container breeding mosquito risk

prediction. Med. Vet. Entomol. 25, 268–275. https://doi.org/10.1111/j.1365-2915.2010.00935.x.

Kraemer, M.U., Sinka, M.E., Duda, K.A., Mylne, A.Q., Shearer, F.M., Barker, C.M., Moore, C.G., Carvalho, R.G., Coelho, G.E., Bortel, W.V., Hendrickx, G., Schaffner, F., Elyazar, I.R., Teng, H.J., Brady, O.J., Messina, J.P., Pigott, D.M., Scott, T.W., Smith, D.L., Wint, G.W., Golding, N., Hay, S.I., 2015. The global distribution of the arbovirus vectors *Aedes aegypti* and *Ae. albopictus*. eLife 4, e08347. https://doi.org/10.7554/eLife.08347.

Kraemer, M.U.G., Reiner, R.C., Brady, O.J., Messina, J.P., Gilbert, M., Pigott, D.M., Yi, D., Johnson, K., Earl, L., Marczak, L.B., Shirude, S., Weaver, N.D., Bisanzio, D., Perkins, T.A., Lai, S., Lu, X., Jones, P., Coelho, G.E., Carvalho, R.G., Bortel, W.V., Marsboom, C., Hendrickx, G., Schaffner, F., Moore, C.G., Nax, H.H., Bengtsson, L., Wetter, E., Tatem, A.J., Brownstein, J.S., Smith, D.L., Lambrechts, L., Cauchemez, S., Linard, C., Faria, N.R., Pybus, O.G., Scott, T.W., Liu, Q., Yu, H., Wint, G.R.W., Hay, S. I., Golding, N., 2019. Past and future spread of the arbovirus vectors *Aedes aegypti* and *Aedes albopictus*. Nature Microbiology 4, 854. https://doi.org/10.1038/s41564-019-0376-y.

Liu, C., Berry, P.M., Dawson, T.P., Pearson, R.G., 2005. Selecting thresholds of occurrence in the prediction of species distributions. Ecography 28, 385–393. https://doi.org/10.1111/j.0906-7590.2005.03957.x.

Liu, C., White, M., Newell, G., 2013. Selecting thresholds for the prediction of species occurrence with presence-only data. J. Biogeogr. 40, 778–789. https://doi.org/10.1111/jbi.12058.

Liu-Helmersson, J., Brännström, Åke, Sewe, M.O., Semenza, J.C., Rocklöv, J., 2019. Estimating past, present, and future trends in the global distribution and abundance of the arbovirus vector aedes aegypti under climate change scenarios. Frontiers in Public Health 7. https://doi.org/10.3389/fpubh.2019.00148.

Merow, C., Smith, M.J., Silander, J.A., 2013. A practical guide to MaxEnt for modeling species' distributions: what it does, and why inputs and settings matter. Ecography 36, 1058–1069. https://doi.org/10.1111/j.1600-0587.2013.07872.x.

Moreno-Madriñán, M.J., Crosson, W.L., Eisen, L., Estes, S.M., Estes Jr., M.G., Hayden, M., Hemmings, S.N., Irwin, D.E., Lozano-Fuentes, S., Monaghan, A.J., Quattrochi, D., Welsh-Rodriguez, C.M., Zielinski-Gutierrez, E., 2014. Correlating remote sensing data with the abundance of pupae of the dengue virus mosquito vector, *Aedes aegypti*, in Central Mexico. ISPRS Int. J. Geo-Inf. 3, 732–749. https://doi.org/10.3390/ijgi3020732.

Ostfeld, R., Glass, G., Keesing, F., 2005. Spatial epidemiology: an emerging (or re-emerging) discipline. Trends Ecol. Evol. 20, 328–336. https://doi.org/10.1016/j.tree.2005.03.009.

Philbert, A., Ijumba, J.N., 2013. Preferred breeding habitats of *Aedes Aegypti* (diptera-culicidae) mosquito and its public health implications in Dar es Salaam, Tanzania. Journal of Environmental Research and Management 4, 344–351.

Phillips, S., Anderson, R., Schapire, R., 2006. Maximum entropy modeling of species geographic distributions. Ecol. Model. 190, 231–259. https://doi.org/10.1016/j.ecolmodel.2005.03.026.

Phillips, S.J., Anderson, R.P., Dudík, M., Schapire, R.E., Blair, M.E., 2017. Opening the black box: an open-source release of maxent. Ecography 40, 887–893. https://doi.org/10.1111/ecog.03049.

Porcasi, X., Andreo, V., Aguirre, E., Rojas, N., Rubio, J., Frutos, N., Guzman, C., Lopez, L., 2019. Spatial analysis of *Aedes aegypti* activity for public health surveillance. In: 2019 XVIII Workshop on Information Processing and Control (RPIC), pp. 214–217. https://doi.org/10.1109/RPIC.2019.8882135.

Porcasi, X., Rotela, C.H., Introini, M.V., Frutos, N., Lanfri, S., Peralta, G., Elia, E.A.D., Lanfri, M.A., Scavuzzo, C.M., 2012. An operative dengue risk stratification system in Argentina based on geospatial technology. Geospatial Health 6.

Powell, J.R., Tabachnick, W.J., 2013. History of domestication and spread of *Aedes aegypti* - a review. Mem. Inst. Oswaldo Cruz 108, 11–17. https://doi.org/10.1590/0074-0276130395.

van Proosdij, A.S.J., Sosef, M.S.M., Wieringa, J.J., Raes, N., 2016. Minimum required number of specimen records to develop accurate species distribution models. Ecography 39, 542–552. https://doi.org/10.1111/ecog.01509.

R Core Team, 2019. R: A Language and Environment for Statistical Computing. R Foundation for Statistical Computing, Vienna, Austria. https://www.R-project.org/.

Reiter, P., Amador, M.A., Anderson, R.A., Clark, G.G., 1995. Short report: dispersal of *Aedes aegypti* in an urban area after blood feeding as demonstrated by rubidium-marked eggs. Am. J. Trop. Med. Hyg. 52, 177–179. https://doi.org/10.4269/ajtmh.1995.52.177.

Rey, J.R., Nishimura, N., Wagner, B., Braks, M.A.H., Lounibos, L.P., 2007. Habitat segregation of mosquito arbovirus vectors in south Florida. J. Med. Entomol. 43, 1134–1141.

Rojas, M.N.R., Lopez, L., Guzman, C., Scavuzzo, C.M., Porcasi, X., Lanfri, M., Aguirre, E., Ferreyra, M.F.G., Lighezzolo, A., Albornoz, C., 2017. Use of geospatial tools for decision-making in the arboviruses prevention and control, in the Córdoba city, Argentina. In: 2017 XVII Workshop on Information Processing and Control (RPIC), IEEE, pp. 1–5. https://doi.org/10.23919/RPIC.2017.8214360.

Rotela, C., 2013. Desarrollo de Modelos e Indicadores Remotos de Riesgo Epidemiológico de Dengue en Argentina. Phd thesis. Universidad de Córdoba.

Rotela, C., Lopez, L., Céspedes, M.F., Barbas, G., Lighezzolo, A., Porcasi, X., Lanfri, M.A., Scavuzzo, C.M., Gorla, D.E., 2017. Analytical report of the 2016 dengue outbreak in córdoba city, Argentina. Geospatial Health. https://doi.org/10.4081/gh.2017.564.

Rubio, A., Cardo, M.V., Vezzani, D., Carbajo, A.E., 2020. Aedes aegypti spreading in South America: new coldest and southernmost records. Mem. Inst. Oswaldo Cruz 115, e190496. https://doi.org/10.1590/0074-02760190496. https://www.ncbi.nlm.nih.gov/pmc/articles/PMC7207151/.

de Santana Martins Rodgers, M., Bavia, M.E., Fonseca, E.O.L., Cova, B.O., Silva, M.M.N., Carneiro, D.D.M.T., Cardim, L.L., Malone, J.B., 2019. Ecological niche models for sand fly species and predicted distribution of *Lutzomyia longipalpis* (diptera: Psychodidae) and visceral leishmaniasis in bahia state, Brazil. Environ. Monit. Assess. 191 https://doi.org/10.1007/s10661-019-7431-2.

Seijo, A., Romer, Y., Espinosa, M., Monroig, J., Giamperetti, S., Ameri, D., Antonelli, L.G., 2009. [outbreak of indigenous dengue in the buenos aires metropolitan area. experience of the f. j. muñiz hospital]. Medicina 69, 593–600.

Servicio Meteorologico Nacional, 2019. Estadísticas climáticas. Ciudad de Córdoba. https://www.smn.gob.ar/estadisticas.

Soberon, J., Peterson, A.T., 2005. Interpretation of models of fundamental ecological niches and species' distributional areas. Biodivers. Inf. 2 https://doi.org/10.17161/bi.v2i0.4.

Soucy, J.P.R., Slatculescu, A.M., Nyiraneza, C., Ogden, N.H., Leighton, P.A., Kerr, J.T., Kulkarni, M.A., 2018. High-resolution ecological niche modeling of *Ixodes scapularis* ticks based on passive surveillance data at the northern frontier of lyme disease emergence in north America. Vector Borne Zoonotic Dis. 18, 235–242. https://doi.org/10.1089/vbz.2017.2234.

Souza-Neto, J.A., Powell, J.R., Bonizzoni, M., 2019. *Aedes aegypti* vector competence studies: a review. Infect. Genet. Evol. 67, 191–209. https://doi.org/10.1016/j.meegid.2018.11.009.

Stanaway, J.D., Shepard, D.S., Undurraga, E.A., Halasa, Y.A., Coffeng, L.E., Brady, O.J., Hay, S.I., Bedi, N., Bensenor, I.M., Castañeda-Orjuela, C.A., Chuang, T.W., Gibney, K. B., Memish, Z.A., Rafay, A., Ukwaja, K.N., Yonemoto, N., Murray, C.J.L., 2016. The global burden of dengue: an analysis from the global burden of disease study 2013. Lancet Infect. Dis. 16, 712–723. https://doi.org/10.1016/S1473-3099(16)00026-8.

Tsuda, Y., Suwonkerd, W., Chawprom, S., Prajakwong, S., Takagi, M., 2006. Different spatial distribution of *Aedes aegypti* and *Aedes albopictus* along an urban-rural gradient and the relating environmental factors examined in three villages in Northern Thailand. J. Am. Mosq. Contr. Assoc. 22, 222–228. https://doi.org/10.2987/8756-971X(2006)22[222:DSDOAA]2.0.CO;2.

VanDerWal, J., Falconi, L., Januchowski, S., Shoo, L., Storlie, C., 2019. SDMTools: Species Distribution Modelling Tools. https://CRAN.R-project.org/package=SDMTools. r package version 1.1-221.1.

Vanwambeke, S.O., Lambin, E.F., Eichhorn, M.P., Flasse, S.P., Harbach, R.E., Oskam, L., Somboon, P., van Beers, S., van Benthem, B.H.B., Walton, C., Butlin, R.K., 2007. Impact of land-use change on dengue and malaria in northern Thailand. EcoHealth 4, 37–51. https://doi.org/10.1007/s10393-007-0085-5.

Verdonschot, P.F.M., Besse-Lototskaya, A.A., 2014. Flight distance of mosquitoes (culicidae): a metadata analysis to support the management of barrier zones around rewetted and newly constructed wetlands. Limnologica 45, 69–79. https://doi.org/10.1016/j.limno.2013.11.002.

Vezzani, D., 2007. Review: artificial container-breeding mosquitoes and cemeteries: a perfect match. Trop. Med. Int. Health 12, 299–313. https://doi.org/10.1111/j.1365-3156.2006.01781.x.

Vezzani, D., Carbajo, A.E., 2008. *Aedes aegypti, Aedes albopictus*, and dengue in Argentina: current knowledge and future directions. Mem. Inst. Oswaldo Cruz 103, 66–74. https://doi.org/10.1590/S0074-02762008005000003.

Vignali, S., Barras, A., Braunisch, V., 2019. SDMtune: species distribution model selection. https://github.com/ConsBiol-unibern/SDMtune. r package version 0.2.0.9000.

Vignali, S., Barras, A.G., Arlettaz, R., Braunisch, V., 2020. SDMtune: an R package to tune and evaluate species distribution models. Ecology and Evolution 00 1–18. https://doi.org/10.1002/ece3.6786. https://onlinelibrary.wiley.com/doi/abs/10.1002/ece3.6786.

Wilke, A.B.B., Chase, C., Vasquez, C., Carvajal, A., Medina, J., Petrie, W.D., Beier, J.C., 2019. Urbanization creates diverse aquatic habitats for immature mosquitoes in urban areas. Sci. Rep. 9 https://doi.org/10.1038/s41598-019-51787-5.